Scale Space Hierarchy

Arjan Kuijper
Luc M.J. Florack
Max A. Viergever

UU-CS-2001-19
June, 2001

Scale Space Hierarchy

Arjan Kuijper * Luc M.J. Florack † Max A. Viergever ‡

Abstract

We investigate the deep structure of a scale space image. We concentrate on scale space critical points – points with vanishing gradient with respect to both spatial *and* scale direction. We show that these points are always saddle points. They turn out to be extremely useful, since the iso-intensity manifolds through these points provide a scale space hierarchy tree and induce a "pre-segmentation": a segmentation without a priori knowledge. Furthermore, both these scale space saddles and the so-called catastrophe points form the critical points of the parameterised critical curves – the curves along which the spatial critical points move in scale space. This enables one to localise these two types of special points relatively easy and automatically. Experimental results concerning the hierarchical representation and pre-segmentation are given and show results that correspond to a fair degree to both the mathematical and the intuitive forecast.

keywords: scale space, catastrophe theory, critical points, topology, deep structure, multi-scale segmentation.

1 Introduction

1.1 Scale Space

One way to understand the structure of an image is to embed it in a one-parameter family. If a scale-parametrised Gaussian filter is applied, the parameter can be regarded as the "scale" or the "resolution" at which the image is observed. The resulting structure has become known as *linear*, or *Gaussian, scale space*. In view of the rich literature on this subject we will henceforth assume familiarity with the basics of Gaussian scale-space theory [11, 18, 25, 36, 43, 47, 49, 54, 55, 57].

1.2 Deep Structure

In their original accounts both Koenderink [25] and Witkin [57] proposed to investigate the "deep structure" of an image, *i.e. structure at all levels of resolution simultaneously*.

*Utrecht University, Department of Computer Science, Padualaan 14, NL-3584 CH Utrecht, The Netherlands. Email: arjan@cs.uu.nl

†Technical University Eindhoven, Department of Biomedical Engineering, Den Dolech 2, NL-5600 MB Eindhoven, The Netherlands. Email: L.M.J.Florack@tue.nl

‡Image Sciences Institute, University Medical Centre Utrecht, E01.334, Heidelberglaan 100, NL-3584 CX Utrecht, The Netherlands. Email: max@isi.uu.nl

Encouraged by the results in specific image analysis applications, an increasing interest has recently emerged in trying to establish a generic underpinning of deep structure. This may serve as a basis for a diversity of multiresolution schemes. Such bottom-up approaches often rely on *catastrophe theory* [1, 14, 38, 44, 50, 51], which is now fairly well-established in the context of the scale-space paradigm.

1.3 Related Work

The application of catastrophe theory in Gaussian scale space has been studied by Damon [8]—probably the most comprehensive account on the subject—as well as by many others [15, 16, 19, 20, 21, 22, 23, 26, 27, 28, 29, 30, 33, 34, 35, 36, 41, 45].

An important stage in using the deep structure is to link image properties of two subsequent resolution scales. Although this may seem obvious, it is a non-trivial task in a discrete scale space. For example, if extrema at different scales correspond to an extremum at the input image, they should be linked. However, extrema may be annihilated or created. Tracking over scale therefore needs a cautious approach.

Koenderink [25] mentioned a possible linking strategy using the properties of the Gaussian scale space. Only a few heuristic attempts have been made to build such multi-scale datastructures.

Vincken et al. constructed a hyperstack segmentation algorithm [52]. Simmons et al. [46] used the idea of Koenderink's scheme for building a so-called extremum stack. Their work was an extension of the results by Lifshitz and Pizer [33], who implemented Koenderink's scheme, mainly focusing on heuristics and the performance of the algorithm.

The idea of tracing critical points and using the location where they vanish as input for a hierarchy tree was also proposed and implemented by Zhao and Iijima [58], cited in [56], and by Wada and Sato [53].

Olsen implemented a segmentation algorithm based on multi-scale watersheds [40, 41, 42].

These datastructures generally use the property of annihilation of extrema at increasing scale. However, the possibility of creations is ignored and consequently not implemented.

As an outcome of the use of catastrophe theory, much effort has been put into investigation of annihilations. It has commonly been accepted that these special points form the crux in understanding the deep structure, although it is not clear how to use them. It has been argued by several authors [17, 25, 33, 35, 36], to use the intensity at the annihilation point.

1.4 Aim

The aim of this paper is to investigate the deep structure of Gaussian scale spaces. We show that this results in an unambiguous hierarchical representation of an arbitrary image. For that reason we combine knowledge from catastrophe theory, the multi-scale linking strategy as suggested by Koenderink [25], and properties of linear scale space. For that reason we introduce the so-called scale space saddles. In section 2 we show that these scale space saddles are the key to explore the deep structure of scale space

images. They give rise to an unambiguous multi-scale hierarchy describing the image. Images in one dimension fundamentally differ from those in higher dimensions, since only in 1D images the scale space saddles coincide with the catastrophe points. Therefore both cases are discussed separately. In appendix A we clarify the theory by discussing the generic annihilation event and the appearance of scale space saddles in its neighbourhood. The scale space saddle approach leads to a non-heuristic hierarchical multi-scale data structure and a segmentation of images without any a priori knowledge and is presented in Section 3. Several examples of our approach on simple artificial images and a 2D MR image are shown in Section 4. Main conclusions and results are given in section 5.

2 Theory

The linearity of a Gaussian scale space enables us to treat the scale parameter as a special variable. For that purpose we describe in this section relevant results known from the literature (Section 2.1) and present new theory based on the critical points in scale space (Section 2.2), critical curves (Section 2.3), and iso-intensity manifolds (Section 2.4), for which purpose we need the following definitions:

Definition 1 $L(\mathbf{x}), \mathbf{x} \in I\!R^n$, *denotes an arbitrary* n*-dimensional image. We will refer to this image as the* initial image.

Definition 2 $L(\mathbf{x};t), (\mathbf{x};t) \in (I\!R^n; I\!R^+)$ *denotes the* $(n+1)$*-dimensional* Gaussian scale space image *of* $L(\mathbf{x})$*, i.e.* $\lim_{t\downarrow 0} L(\mathbf{x};t) = L(\mathbf{x})$.

Definition 3 *Spatial critical points, i.e. saddles and extrema (maxima or minima), at a certain scale* t_0 *of* $L(\mathbf{x};t)$ *are defined as the points at fixed scale* t_0 *where the spatial derivatives vanish:* $\nabla L(\mathbf{x};t_0) = \mathbf{0}$*. We will refer to these points as* spatial critical points *to distinguish them from scale space critical points, see Definition 4.*

Definition 4 *Scale space critical points of* $L(\mathbf{x};t)$ *are defined as the points where both the spatial derivatives and scale derivative vanish:* $\nabla L(\mathbf{x};t) = \mathbf{0}$ *and* $\partial_t L(\mathbf{x};t) = 0$*. Since for Gaussian scale spaces the diffusion equation holds, the latter equation equals* $\Delta L(\mathbf{x};t) = 0$*, denoting a zero Laplacean. We will refer to these points as* scale space critical points.

Definition 5 *A* critical curve *is a one dimensional manifold in the* $(\mathbf{x};t)$ *(scale) space on which* $\nabla L(\mathbf{x};t) = \mathbf{0}$*. The intersection of all critical curves with a certain scale space level* t_0 *results in the spatial critical points of* $L(\mathbf{x};t_0)$.

Definition 6 *The* Hessian *is the matrix of second order spatial derivatives:* $H = \nabla\nabla^T L$.

Definition 7 *A* branch of a critical curve *is a subset of a critical curve on which the sign of determinant of the Hessian doesn't change.*

Definition 8 *A* Iso-intensity manifold *is an* n*-dimensional manifold in the* $(\mathbf{x};t)$ *scale space on which* $L(\mathbf{x};t) = c, c \in I\!R$.

2.1 Deep Structure in Gaussian Scale Space

2.1.1 Catastrophe theory

The behaviour of critical points as the (scale) parameter changes is described by catastrophe theory. As the parameter continuously changes, the critical points move along critical curves. If the determinant of the Hessian does not become zero, these critical points are called *Morse critical points*. In a typical image these points are extrema (minima and maxima) or saddles. *The Morse lemma* states that the topology of a neighbourhood of a Morse critical point can essentially be described by a second order polynomial. At isolated points on a critical curve the determinant of the Hessian may become zero. These points are called *non-Morse points*. As described by *Thom's theorem* [50, 51], neighbourhoods of such points need m^{th}-order polynomial, where $m > 2$. These polynomials are called the *catastrophe germs*. If an image is slightly perturbed, the Morse critical points may undergo a small displacement, but qualitatively nothing happens to them. A non-Morse point, however, will change. It will split into a non-Morse point that can be described by a polynomial of lower order and a number of Morse critical points, or solely into Morse critical points. This event is called *morsification*. Thom's theorem provides a list of elementary catastrophes with canonical formulas[1] for the catastrophe germs and the perturbations. The Thom splitting lemma states that *canonical coordinates* exist in which these events can be described. In general, these 'curved' coordinates don't coincide with the user-defined (usually Cartesian) coordinates, but are used for notational convenience. In Gaussian scale space the only generic events are *annihilations* and *creations* of a pair of Morse points: an extremum and a saddle in the 2D case. All other events can be split into a combination of one of these events and one 'in which nothing happens'. See Damon [8] for a proof. Canonical descriptions of these events are given by the following formulae:

$$f^{\mathrm{A}}(\mathbf{x};t) \stackrel{\mathrm{def}}{=} x_1^3 + 6x_1 t + Q(x_2,\ldots,x_n;t) \tag{1}$$

$$f^{\mathrm{C}}(\mathbf{x};t) \stackrel{\mathrm{def}}{=} x_1^3 - 6x_1(x_2^2 + t) + Q(x_2,\ldots,x_n;t), \tag{2}$$

where for all $a_i \neq 0$, Q is defined by

$$Q(x_2,\ldots,x_n;t) \stackrel{\mathrm{def}}{=} \sum_{i=2}^{n} a_i \left(x_i^2 + 2t\right)$$

with $\sum_{i=2}^{n} a_i \neq 0$ and $a_i \neq 0,\ 2 \leq i \leq n$. Note that Eq. (1) and Eq. (2), describing annihilation and creation respectively, satisfy the diffusion equation

$$\frac{\partial L}{\partial t} = \Delta L\,. \tag{3}$$

It can be verified that the form $f^{\mathrm{A}}(x,y;t)$ corresponds to an annihilation at the origin via the critical path $(\sqrt{-2t}\,,\,0\,;\,t)\ ,\ t \leq 0$, and $f^{\mathrm{C}}(x,y;t)$ to a creation via the critical path $(\sqrt{2t}\,,\,0\,;\,t)\ ,\ t \geq 0$.

[1] Notation due to Gilmore [14]. Also the terminology *normal forms* is used in the literature, *e.g.* by Poston and Steward [44].

Note that creations are generic. They are not sometimes temporarily created, nor false extrema, nor pathological cases, although it is true that they are not as frequently encountered as annihilations.

In 1-D images only annihilations occur. Then Eq. (1) becomes $f^{\text{A}}(x;t) \stackrel{\text{def}}{=} x^3 + 6xt$. See *e.g.* Lindeberg [36] for a proof.

2.1.2 Extremum principle and iso-intensity manifolds

A consequence of the Gaussian scale space representation is the strong smoothing property, usually mentioned for its *non-enhancement of local extrema*. It corresponds to the *extremum principle* for parabolic differential equations:

> If at a certain scale $t_0 > 0$ a point $\mathbf{x}_0$ is a local maximum (minimum) of the function $L(\mathbf{x};t_0)$, then the Laplacean $\Delta L(\mathbf{x}_0;t_0)$ at this point is negative (positive). This means that $\partial_t L(\mathbf{x}_0;t_0)$ is strictly negative (positive).

In other words, small local variations will be suppressed. See e.g. Lindeberg [36] or Weickert [54] for more details.

As a result, the structure of iso-intensity manifolds in scale space close to an extremum is dome-shaped: At some scale an extremum, e.g. a maximum, is encapsulated by iso-intensity manifolds (isophotes in 2D), topologically equivalent to spheres (circles in 2D). The intensity of each of these manifolds is smaller than that of the maximum. Due to the extremum principle the intensity of the maximum decreases with increasing scale. At a certain scale the intensity of the maximum will equal the intensity of some manifold. Alternatively, the shape of the intersection of the image at increasing scales and the iso-intensity manifold shrinks until it coincides at certain scale with the maximum and then disappears. In 2D this can easily be visualised by a set of circles contracting to the maximum at increasing scale: that is, the iso-intensity manifold is dome-shaped. The top of the dome corresponds to the disappearance of the iso-intensity manifold around this extremum. See Figure 1 for an example of various iso-intensity manifolds.

Since the image at sufficiently large scale contains only one extremum (see [37]), the evolution of extrema induces a family of iso-intensity domes, nested like onion peels.

2.2 Scale Space Critical Points

Since scale provides an extra dimension to the initial image, interesting features are to be expected from the critical points of the scale space image as defined by Definition 4. In this and the following sections we present novel theory regarding these points.

The scale space critical points are defined as the points in scale space with zero gradient and zero Laplacean:

$$\begin{cases} \nabla L(\mathbf{x};t) &= 0 \\ \Delta L(\mathbf{x};t) &= 0 \end{cases}$$

since $\partial_t L(\mathbf{x};t) \stackrel{\text{def}}{=} \Delta L(\mathbf{x};t)$. The type of these scale space critical points is determined by the eigenvalues of the matrix of second order derivatives in scale space, $\mathcal{H}$. We call

this matrix the *extended Hessian*:

$$\mathcal{H} = \begin{pmatrix} H & \Delta\nabla L \\ (\Delta\nabla L)^T & \Delta\Delta L \end{pmatrix}. \tag{4}$$

Here H is the (spatial) Hessian. All derivatives are evaluated at the location of the scale space critical point of interest. Points are maxima (minima) if all eigenvalues are negative (positive). If at least two eigenvalues have a different sign, the point is a saddle. $\mathcal{H}$ has the following properties:

- Since the matrix $\mathcal{H}$ is symmetric all eigenvalues are real.
- At scale space critical points $\operatorname{tr} H \equiv \Delta L = 0$, so $\operatorname{tr}\mathcal{H} = \Delta\Delta L$.
- $\det\mathcal{H} = \det H\Delta\Delta L - \Big((\Delta\nabla L)^T \tilde{H}\Delta\nabla L\Big)$, where $\tilde{H} \stackrel{\text{def}}{=} \det H \cdot H^{-1}$, the transposed co-factor matrix of H. In fact, this matrix is always well-defined, since its components are homogeneous polynomial combinations of the components of H of degree $n-1$, see [12, 31]. So at catastrophe points $\tilde{H}$ is generically non-zero, although $\det H = 0$. At these points $\det\mathcal{H}$ reduces to $-\Big((\Delta\nabla L)^T \tilde{H}\Delta\nabla L\Big)$, which is equal to the generically non-zero invariant $-\Delta L_i \Delta L_j \tilde{H}_{ij}$ (summation convention applies).
- The determinant of $\mathcal{H}$ can also be written as

  $$\det\mathcal{H} = \big((\Delta\nabla L)^T; \Delta\Delta L\big) \cdot \begin{pmatrix} -\tilde{H}\Delta\nabla L \\ \det H \end{pmatrix}$$

  Here the component $\big((\Delta\nabla L)^T; \Delta\Delta L\big)$ is the normal vector of the plane with constant Laplacean. The component $(-\tilde{H}\Delta\nabla L; \det(H))^T$ denotes the (scale space) tangent of the critical curve in scale space at the spatial critical points. It is always finite in value, even at catastrophe points. See Florack and Kuijper [12, 31] for more details.
- Scale space critical points are always scale space saddle points. See Theorem 1.

Theorem 1 *The matrix $\mathcal{H}$ has both positive and negative eigenvalues at scale space critical points.*

Proof 1 *Let the point $(\mathbf{x}_0; t_0)$ be a scale space critical point of the function $L(\mathbf{x}; t)$. Then $(\mathbf{x}_0; t_0)$ is also a spatial critical point of the function $L(\mathbf{x}; t_0)$ at scale t_0. If $(\mathbf{x}_0; t_0)$ is a scale space extremum of $L(\mathbf{x}; t)$, it is also a spatial extremum of $L(\mathbf{x}; t_0)$. However, the extremum principle (section 2.1.2) states that the Laplacean of a spatial extremum is non-zero, leading to the contradiction that $(\mathbf{x}_0; t_0)$ cannot be a scale space critical point. Therefore $(\mathbf{x}_0; t_0)$ is a scale space saddle point. Consequently, $\mathcal{H}$ has both positive and negative eigenvalues at scale space critical points.* $\square$

As a consequence, critical points in scale space ($\nabla L = 0$ and $\Delta L = 0$) are *always* saddle points. These scale space saddle points form a subset of the spatial saddles, viz. those with vanishing Laplacean.

This property of scale space critical points follows directly from the notion of causality, that states that isophotes in scale space only disappear and never appear (no spurious detail).

The only spatial critical point traversing the scale space saddle is the spatial saddle. Since the manifold $\nabla L = 0$ intersects the manifold $\Delta L = 0$ transversally, the intensity of this spatial saddle has an extremum at the scale space saddle. Therefore, its intensity first increases and then decreases, or vice versa. This is exactly the behaviour Lifshitz and Pizer observed, see [33]. We elaborate on this behaviour in section 2.3 and go into details in appendix A.

2.3 Properties of Critical Curves in Scale Space

According to Definition 7, in scale space each critical curve contains branches representing spatial critical points. Branches are connected at catastrophe points, where two spatial critical points are annihilated or created. These two spatial critical points differ with respect to the sign of one eigenvalue of the Hessian, that becomes zero at the catastrophe. Of all other eigenvalues the number of positive and negative signs is equal. Note that a critical curve can contain several catastrophe points if $n > 1$.

In two-dimensional images the two branches connected at catastrophe points necessarily are a saddle and an extremum branch, in one-dimensional images they are a maximum and a minimum branch. In higher dimensions interactions become more complicated, since catastrophes of saddles of different type are also possible. For writing convenience we will use the terminology appropriate for 2D images: saddle and extremum (minimum, maximum) branches to distinguish between the two types of spatial critical points involved at the catastrophe, but results remain valid for other dimensions.

It is known from catastrophe theory that each branch of the critical curve is bounded with respect to scale: at some scale the spatial critical points annihilate. Spatial critical points are either present from the initial scale or they are created at a certain (catastrophe) point in scale space. If the coarsest scale is taken large enough only one extremum remains. Then the scale space image contains one critical curve bounded by the coarsest scale.

Apart from catastrophe points a second type of points exhibits special behaviour, viz. scale space saddles.

2.3.1 Scale Space Saddles

On an extremum branch the intensities are damped continuously while increasing scale. Each minimum (maximum) intensity therefore increases (decreases) monotonically towards the intensity at the annihilation point. At certain spatial and scale distance from the annihilation, the intensity of corresponding saddle will generally tend to move towards the intensity of extremum, i.e. it decreases (increases) to the intensity of minimum (maximum). So the signs of the Laplacean of both spatial critical points at that scale will be opposite. At the catastrophe point, however, they necessarily have the same sign and both points approach the intensity of the annihilation in a decreasing (increasing) fashion.

This was observed by Griffin, who pointed out that at a catastrophe the saddle and the extremum necessarily have the same sign of the Laplacean. He distinguished between ridge and trough saddles. Saddles may change from 'ridge' (negative Laplacean) to 'trough' (positive Laplacean) or vice versa with increasing scale and generically occur as 'balanced' saddle (zero Laplacean) [15, 16].

Therefore, at the saddle-branch of the critical curves, the saddle will generically pass a point at which the Laplacean equals zero: a scale space saddle. Since the sign of the Laplacean changes while passing the scale space saddle, the intensity on the saddle branch has a local extremum.

2.3.2 Parametrisation

A parametrisation of a critical curve leads to a 1D-function of the intensity of the spatial critical points.

Definition 9 *Let $(\mathbf{x}(s); t(s))$ be a parametrisation of $(\mathbf{x}; t)$, such that $\nabla L(\mathbf{x}(s); t(s)) = 0$, i.e. $(\mathbf{x}(s); t(s))$ defines a critical curve. Then the intensity of the parametrised curve $P(s)$ is defined by $L(\mathbf{x}(s); t(s))$ for a compact range $s \in [s_{\min}; s_{\max}]$.*

Note that $P(s)$ can be a combination of several connected parts $P_i(s_i)$, each defined on a compact interval $[s_{i,\min}; s_{i,\max}]$. Two parts $P_i(s_i), P_j(s_j)$ are connected at a catastrophe point given by either $s_{i,\min} = s_{j,\min}$ or $s_{i,\max} = s_{j,\max}$.

The local extrema of $P(s)$ have the following property:

Theorem 2 *For $n-D$ images, $n > 1$, $P(s)$ has its critical points at the scale space saddle(s) and the catastrophe point(s). They are extrema.*

Theorem 3 *If, for 1D images (signals), the critical point of $P(s)$ is located at the interior of $[s_{\min}; s_{\max}]$, it is a point of inflection.*

Proof 2 *The critical points of $P(s)$ are defined by $\partial_s P(s) = 0$. According to definition 9, the left part of this equation equals the total differentiation of $L(\mathbf{x}(s); t(s))$ with respect to s, defined by*

$$\frac{dL(\mathbf{x}(s); t(s))}{ds} = \nabla L(\mathbf{x}(s); t(s)) \cdot \mathbf{x}_s(s) + \Delta L(\mathbf{x}(s); t(s)) \cdot t_s(s). \tag{5}$$

Here

$$\mathbf{x}_s(s) \stackrel{\text{def}}{=} \frac{d\mathbf{x}}{ds}, \quad t_s(s) \stackrel{\text{def}}{=} \frac{dt}{ds}.$$

Since $\nabla L(\mathbf{x}(s); t(s)) = 0$, the critical points of Eq. (5) are given by $\Delta L(\mathbf{x}(s); t(s)) \cdot t_s(s) = 0$. The scale space saddles are defined as the spatial critical points where $\Delta L(\mathbf{x}(s); t(s)) = 0$. The catastrophes take place at the location where the saddle and the extremum 'meet' in scale space, i.e. where the parametrisation of scale has its local extrema. These points are given by $t_s(s) = 0$.

The critical points of $P(s)$ are extrema, since at the catastrophe point the Laplacean is non-zero for n-D images, $n > 1$. □

Proof 3 *For 1D images the zero-Laplacean and the catastrophe point coincide, so if the critical point lays in the interior of* $[s_{\min}; s_{\max}]$*, the solution of* $t_s(s) = 0$ *equals that of* $\Delta L = 0$*.* $\square$

Although these results holds for any parametrisation of the critical curves, in practice the intensities of spatial critical points are obtained at the calculated scales of the scale space. In other words, they are measured as a function of scale. Then $t = s$, so $t_s = 1$ and $P(s)$ is obtained as the union of parts $P_i(s_i)$ containing the branches of critical points. Each branch is defined on a open interval $s_1 < s < s_2$, where s_1 is either the initial or the creation scale, and s_2 is the annihilation scale of the spatial critical point. The branches are connected at the catastrophe points, emphasising that the detection and use of creations is essential to build accurate critical paths.

In Appendix A we clarify these theorems using generic events in scale space.

2.3.3 Number of Scale Space Saddles

As argued in section 2.3.1, we may generally assume that the intensity at the annihilation of an extremum-saddle pair lays between the intensities of both spatial critical points at a certain scale below the annihilation scale. Then the spatial critical points have opposite signs of Laplacean and the saddle passes a scale space saddle with increasing scale. The number of scale space saddles on a saddle branch of a critical curve is, however, undetermined and the saddle branch of a critical curve can contain zero, one, or multiple scale space saddles.

This was also observed by Lindeberg [35, 36] who investigated the locations of Laplacean zero-crossings in combination with the (annihilation of) critical points concluding that in two and higher dimensions there is no absolute relation between locations of the Laplacean zero-crossing curves and the local extrema of a signal.

Intuitively the case without scale space saddles can be made clear by imagining an image of an extremum and a saddle with (already) the same sign of Laplacean.

Multiple scale space saddles on a saddle branch are caused by changing structure in the image nearby the saddle point.

Examples of this varying number of scale space saddles on a single branch can be found in section 4.2.2.

2.4 The Structure of Iso-intensity Manifolds

The iso-intensity manifolds of a 2D image are formed by the isophotes. These isophotes generally are Jordan curves, i.e. non-intersecting curves. If they don't end on the boundary they are closed, e.g. the isophotes around an extremum. There exist a finite number of non-Jordan curves. These curves do intersect themselves in the (spatial) saddle points of the image. Generically these curves have but one point of self-intersection. Consequently the image is separated into regions in which all isophotes are Jordan curves by the isophotes through the saddle points. This separation can be extended to arbitrary dimension.

The extension to scale space images leads to the necessity of scale space saddle points, as defined in the previous section. The iso-intensity manifolds through these

points form the natural separation of parts of the scale space image. Each spatial extremum can be assigned to a spatial saddle by means of an extremum-saddle catastrophe, and consequently it can be assigned to the scale space saddle corresponding to the spatial saddle, if the saddle branch contains one. Each spatial extremum is encircled by iso-intensity manifolds of which the one through the scale space saddle forms the 'critical' manifold. That is: all iso-intensity manifolds beneath the critical manifold form a closed segment in scale space.

Definition 10 *A scale space segment is defined as a part of a scale space image that is bounded by the dome part of the iso-intensity manifold through a scale space saddle; the top of the dome is a spatial extremum.*

There are four essentially different types of iso-intensity manifolds shown in Figure 1 and explained hereafter:

- Iso-intensity manifolds are dome-shaped and don't intersect themselves. Each dome has its open ends towards finer scale. The top of the dome lays on the extremum branch of the critical curve. Consequently, these domes encapsulate a bounded region in scale space. The dome doesn't intersect nor touch the saddle branch, see Figure 1a.

- The iso-intensity manifold through a scale space saddle consists of two parts, separated by the scale space saddle. One part is dome-shaped around the spatial extremum connected to the scale space saddle by the critical curve. At the scale space saddle this manifold touches another having the same intensity, see Figure 1b.

- Iso-intensity manifolds with intensities between the scale space saddle and the catastrophe point are still dome-shaped around the spatial extremum, but have a 'hole in the roof' around the scale space saddle. Consequently, the maximum scale at which the iso-intensity manifold occurs is not determined by the spatial extremum, see Figure 1c. The saddle branch is intersected twice by the iso-intensity manifold. In fact, the manifold transforms from dome-shaped to horseshoe as described in the next item.

- The iso-intensity manifold through a catastrophe point has a horseshoe shape, as is known from catastrophe theory. It touches the critical curve at the catastrophe point, see Figure 1d.

As a dual expression it follows that starting from the initial image, spatial extrema on a extremum branch of a critical curve form the top of a dome-shaped iso-intensity manifold in scale space that doesn't intersect itself and is present at all scales beneath the scale at which the spatial extremum occurs, until its intensity equals that of a scale space saddle on the saddle branch of the critical curve. Increasing scale, *i.e.* tracking the extremum further on the extremum branch, the iso-intensity manifold through the spatial extremum transforms to a horseshoe shape at the annihilation. In case of a minimum (maximum) there are only a pure domes at intensities smaller (larger) than the intensity of the scale space saddle.

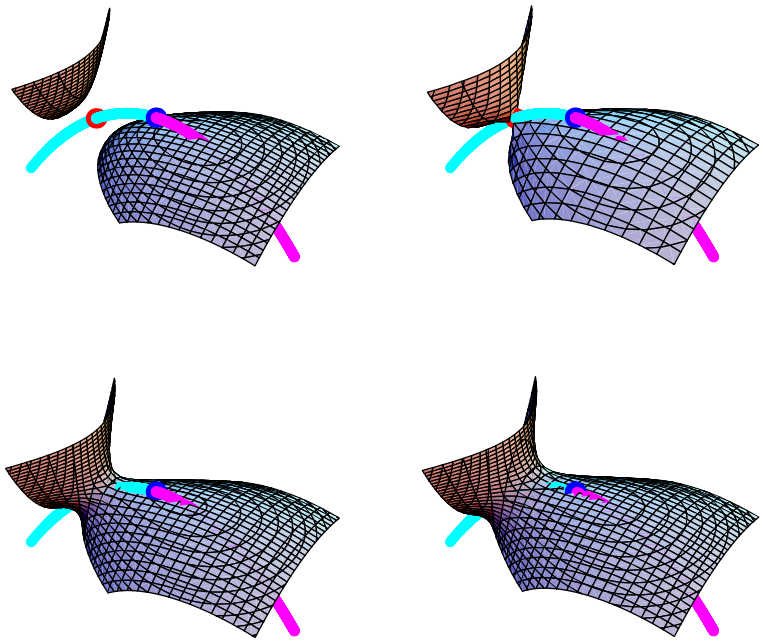

Figure 1: Intersections of 2D Iso-intensity surfaces and the critical curve a) Dome-shaped – one intersection b) Through the scale space saddle, two touching manifolds – two intersections c) Dome-with-hole: intensities between the scale space saddle and the catastrophe point – three intersections d) Horseshoe surface through the catastrophe point – two intersections

3 Scale Space Hierarchy and Pre-Segmentation

In the previous section we have given a theoretical framework in which iso-intensity manifolds defined scale space segments. The manifolds through scale space saddles can be regarded as separatrices of these segments. By definition, each of the scale space segments contains at least one extremum. If a segment contains multiple extrema, it obviously contains subsegments. Consequently, the set of scale space saddles and their iso-intensity manifolds induce both a hierarchy and a segmentation of the scale space image. These two properties are discussed in detail in the following subsections.

3.1 Scale Space hierarchy

A natural hierarchy results as scale space segments are defined by the regions encapsulated by the iso-intensity manifolds through the scale space saddles. This hierarchy avoids problems arising when defining a straight-forward and non-multiscale hierarchy of an image based solely on the nesting of iso-intensity contours through the spatial saddle points in the initial image. Although this nesting defines a hierarchy at some scale, it is not scale independent. Generically, spatial saddles have different intensities in the initial image since they are Morse-saddles. When scale is increased the nesting can change: At some scale levels intensities of saddles become equal. Then, for example, the isophote through a saddle contains another saddle and encircles three extrema. They form the so-called Maxwell set. Increasing scale, the nesting of the saddles swaps, see e.g. Lindeberg [36].

Since scale space saddles generically have different intensities, a unique scale space hierarchy is found using the nesting of the scale space saddle, as described by the following algorithm:

Scale Space With the input of an n-D image, build a scale space consisting of $k+1$ levels, $t = 0, 1, \ldots, k$.

Extremum and Saddle Stacks Find the extrema and the saddle points at each level t together with their intensities and put them in two separate stacks.

Extremum and Saddle Branches Link each critical point location at level t to its corresponding location at level $t+1$, $t = 0, \ldots, k-1$ *and* vice versa, as long as this successive location is found. This results in doubly linked lists of critical points in each stack.

Connected Critical Paths For each list in the extremum stack find a list in the saddle stack and combine them pairwise to critical curve lists by means of these catastrophe points.

Scale Space Saddles Find the scale space saddles and their intensities along each critical curve, i.e. find the intensity extrema of each saddle list.

Hierarchical Tree Sort the catastrophe points from coarse to fine scales and construct the hierarchy tree starting at highest scale. While descending in scale, each successive catastrophe denotes a critical curve with a scale space saddle and thus

defines a new segment of the hierarchy tree as a sub-segment of an existing segment. That is, one branch of the tree is split into two branches in a unique way.

In the following sections these items will be explained and illustrated.

3.1.1 Scale Space

Input is a discrete image of arbitrary size and dimension. Only for the sake of illustration we consider the one- and two-dimensional cases. Images of higher dimension are comparable to the two-dimensional ones, albeit that they allow saddle-saddle pairs at catastrophes. These pairs, however, behave equivalently to saddle-extremum pairs.

A scale space image is obtained by convolving the input image with a normalised Gaussian filter of variable size. The intermediate levels are logarithmically sampled, see e.g. [11, 25, 30, 36, 39, 47, 48, 49].

3.1.2 Extremum and Saddle Stacks

Each level in scale space is a blurred image. Its spatial critical points can be calculated by various methods, e.g. zero-crossings of the derivatives, winding-numbers (see [23]), or neighbourhood-relations. The latter has several implementations. For 2-D images Bloms method [3, 4] may be preferred. This method uses a hexagonal lattice based scheme, in which the intensity of each point is compared to its 6 neighbours. The advantage of this scheme is that it finds all the saddle points and 'respects' the Euler number. Common pixel-based methods like the 4- and 8-neighbourhood schemes sometimes miss saddles or cluster them. However, the generalisation of Bloms method to higher dimensions is non-trivial.

Critical point locations and their intensities are stored in two stacks, one containing the saddles and one containing the extrema.

3.1.3 Extremum and Saddle Branches

Since critical points can be annihilated and created, they inherit both movement in increasing scale direction and spatial drift. This scale space movement can be calculated accurately by means of derivatives up to third order, see e.g. [12, 31] and gives the expected location of the spatial critical point at the next scale.

So to each spatial critical point $\mathbf{x}_{i,t}$ at level t its expected location $\mathbf{x}^e_{i,t+1}$ at level $t+1$ is assigned. To link spatial critical points at two subsequent levels, the point sets $\mathbf{x}_{i,t}$ and $\mathbf{x}^e_{i,t+1}$ are compared to the critical points $\mathbf{x}_{j,t+1}$ at the next level. We define the distance matrices $d^1_{i,j}$ and $d^2_{i,j}$ by

$$\left\{ \begin{array}{lcl} d^1_{i,j} & = & \| \mathbf{x}_{i,t} - \mathbf{x}_{j,t+1} \|, \\ d^2_{i,j} & = & \| \mathbf{x}^e_{i,t+1} - \mathbf{x}_{j,t+1} \| , \end{array} \right.$$

and set $d_{i,j} = \min(d^1_{i,j}, d^2_{i,j})$. Next, we take $\min_{i,j} d_{i,j}$, establishing a link, and remove the row and column containing this value. The linking continues until either all points at level $t+1$ are linked (and the matrix d has zero rank), or $\min d_{i,j}$ exceeds scale.

The outcome of this procedure are two stacks each containing doubly linked lists. The head of each list corresponds with the creation of the critical point (or the initial scale), its tail with the annihilation.

3.1.4 Connected Critical Paths

Since the annihilation of an extremum involves a saddle, each tail of an extremum list at a certain scale t corresponds to a tail of some saddle list at the same scale t. the same holds for creations in relation to the heads of the lists.

Note that at catastrophes the spatial drift becomes undetermined since $\det(H) = 0$. Then the movement of a critical point can still be accurately predicted, see [12, 31].

Relating saddle and extremum lists results in chains of extremum-saddle sets, viz. critical curves.

3.1.5 Scale Space Saddles

Scale space saddles have the property that they are the local extrema of the parametrised intensity-curve, obtained by taking the intensity along the saddle branches as function of scale, as argued in section 2. They are easily found by a list-operation on the saddle lists. Saddle lists can have zero or multiple extrema with respect to intensity.

If no extrema are found then the Laplaceans of the extremum and the saddle have either the same or the opposite sign at all scales on which their are found. The former signals that there was no scale space saddle in the range of used scales. One might say that it is located at a scale that is smaller than the scale of the first image of the scale space stack. To identify a segment with the extremum, the intensity of the saddle in that first image can be taken. The latter case represents a scale space saddle located closer to the catastrophe point than resolutions allows to be measured. Then the saddle at the coarsest scale is assigned as scale space saddle.

If multiple scale space saddles are found within one saddle list, the one with maximum (minimum) intensity in case of a minimum (maximum)is chosen.

Since each extremum list is linked to a saddle list, each extremum is linked to a scale space saddle containing the global intensity extremum in the the saddle list. Equivalently, the iso-intensity manifold through the scale space saddle encapsulates the corresponding extremum.

3.1.6 Hierarchical Tree

The annihilations –and consequently each extremum branch– are sorted from coarse to fine scale. Each scale space saddle defines an iso-intensity manifold around an extremum: the part of the image encapsulated by this manifold is a segment of the image at that scale. Segments may have sub-segments, defined by scale space saddles within the segment.

At the coarsest scale only one extremum remains. Since it has no corresponding saddle branch containing a scale space saddle, it doesn't have an a priori critical dome. Without the presence of a saddle the iso-intensity manifolds through an extremum is

obviously dome-shaped. Therefore the iso-intensity manifold of the remaining extremum can be chosen having the intensity of the extremum at the coarsest scale. Since the heat equation is energy preserving, it is known that the input image converges to an image of constant value equalling the average value of the input image. Consequently the value of the iso-intensity manifold of the remaining extremum can be set to this value.

The hierarchy tree contains as nodes the locations of the annihilations in scale space, together with their corresponding scale space saddles and their intensities. The branch to the parent corresponds to the scale space segment in which the scale space saddle is located. The branches to the children of the tree are formed by the original segment and the new segment defined by the scale space saddle. The root of the tree is defined as the one remaining extremum.

3.2 Segmentation

A natural segmentation of *scale space* is thus obtained by the iso-intensity manifolds of the scale space saddles with their corresponding extrema. Consequently, a *spatial* segmentation, or rather "pre-segmentation", of the image at any scale t is found by the intersection of the scale space segmentation and the image at this fixed scale t. A full (partial) pre-segmentation of the initial image is found by taking into account the intensities of all (a subset of all) scale space saddles. The word "pre-segmentation" is used to distinguish between the proposed separation of the image into topologically different parts and the commonly user-defined (and user-verified) segmentations. The latter introduce by definition prior knowledge and are therefore definitely different from our proposed pre-segmentation.

At a partial segmentation each selection of scale space saddles defines segments of the image within some grey-level range in the part of the image enclosed by the iso-intensity manifold. Knowledge of the grey-level distribution of the image may then lead to a semantical choice of scale space saddles and their corresponding segments and thus using the pre-segmentation as a pre-stage for the "real" user-defined segmentation. This partial segmentation is easily obtained by elementary tree operations, e.g. selecting or deselecting subtrees, contracting nodes in the tree, etc.

Finally, to obtain a rough segmentation, that is a segmentation based on the large structures, only the upper part of the tree with large scales can be taken into account.

4 Applications

In this section we apply the algorithm as described in the previous section to a 1D signal and to two 2D images. We present the obtained hierarchy trees and show pre-segmentations. We also give an illustration of the effect of tree operations on the pre-segmentation.

Figure 2: 1D signal at increasing scale: a) Initial signal b) After the first catastrophe, c) after the second catastrophe, d) and after the last catastrophe.

4.1 1D signals

As first example we use the part of a 1D signal shown in Figure 2a. As can be seen directly, it contains three minima and three maxima, so the scale space image contains three scale space saddles (equivalently: catastrophes, annihilations). The four topologically different appearances of this signal in scale space after successive catastrophes are shown in Figure 2a-d.

The scale space hierarchy tree is shown in Figure 3. At high scales there is only one segment S_0: the whole image from boundary to boundary, as shown on the top-right side of Figure 3. Decreasing scale, one reaches scale space saddle 3, from which point the image contains two segments: S_1 and the complement of S_1: the parts that range from the boundaries to S_1. Continuing the descent one reaches scale space saddle 2, from which point segment S_1 contains a subsegment, viz. S_2. Decreasing scale even more one ends up with scale space saddle 1, from which point a new segment S_3 is obtained from the boundary part.

Interpreting Figure 3 the other way round one concludes that starting with the pre-segmentation where $S_2 \subset S_1 \subset S_0,\ S_3 \subset S_0$ at increasing scale firstly segment S_3 vanishes at the boundary, secondly S_2 is "gulped down" by S_1 , and finally S_1 disappears.

The notion of disappearing of structure at annihilation points gave rise to the gist that the essence of segmenting images should be based on catastrophe points instead of scale space points. This misinterpretation is caused by the coincidence of scale space saddles and catastrophe points in 1D.

4.2 2D images

As 2D examples we firstly took an 81x81 artificial image, built up by the combination of four Gaussian blobs, see Figure 4a. Note that the four maxima induce one minimum. The simplicity of this image enables a quantitative check of the outcome. Subsequently we took a 2D slice from an artificial MR image shown in Figure 4b to illustrate the use and possibilities of the hierarchy tree. This image is taken from the *Brain Web* [6, 7, 32], web site http://www.bic.mni.mcgill.ca/brainweb.

4.2.1 Artificial image

The 81 x 81 artificial image contains five extrema. Since the image at (very) large scale contains only one blob, four extrema must be annihilated. To obtain the scale space hierarchy a scale space consisting of 113 levels was built. Levels were calculated at

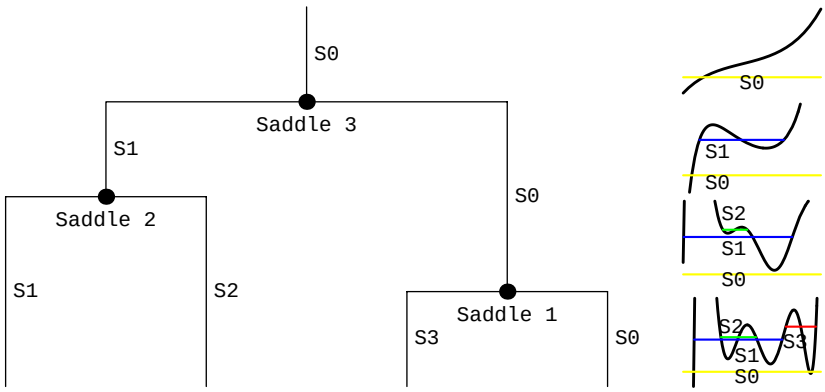

Figure 3: Left: Hierarchy tree of Figure 2a, at the top coarsest scale. The three 'Saddles' denote the subsequent topological changes (catastrophes, annihilations) of the image as scale increases. The vertical branches denote the distinguished segments present at these scales. The stack of images at the right show the shape of the signal, changing at the three scale space saddle scales, and their pre-segmentations.

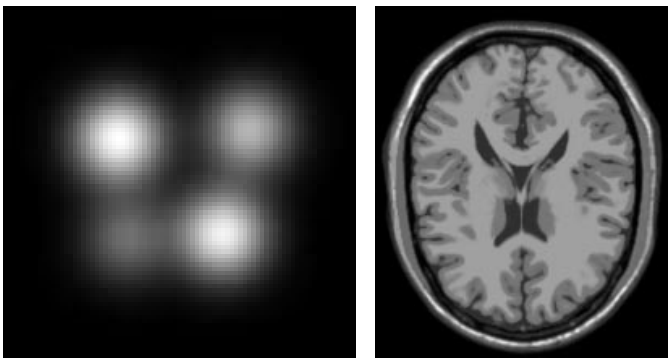

Figure 4: 2D test images Left: Artificial image built by combining four maxima and one minimum. Right: 181 x 217 artificial MR image.

scales $e^{i/32}, i = 2, \ldots, 114$ and at each level the spatial critical points were calculated. Figure 5 shows 15 levels of the stack at increasing scales together with the calculated spatial critical points.

Next, the spatial critical points of subsequent scales were linked resulting in the critical paths. Figure 6 shows the locations of spatial critical points in scale space. For visualisation purposes this 81x81x113 scale space was reduced to a 41x41x113 volume of interest space, since the critical points evolve in the middle of the image so a spatial border of 20 pixels was omitted. Dark grey points correspond to extrema, light grey points to saddle points. We note that at three isolated scales a pair of created and directly annihilated critical points were detected. The algorithm is able to detect these points and proposes the right linking.

The parametrised critical paths, viz. the intensities of the critical curves containing the branches of saddle and extremum branches, are shown in Figure 7. The top row shows the branches of the saddles (left) and the extrema (right). Since the detection of critical points only takes place at pixel-level, the saddle intensities sometimes show discontinuous behaviour at spatial movement. The extrema and saddle points were pairwise grouped by means of the catastrophe points. Annihilations occur at $t = 48, 55, 66, 77$, i.e. at scales 4.48, 5.58, 7.87, and 11.1. The four catastrophes are visible as the end of two branches of critical points. At these points saddle and extremum branches are connected forming the critical paths, see the bottom row of Figure 7. On the left all critical curves are shown, on the right one saddle-extremum pair is taken apart.

The scale space saddles are derived from the saddle branches. It can be seen that the upper three saddle branches shown in Figure 7, although containing multiple local extrema with respect to the intensity, have a global maximum, viz. the scale space saddle of interest. The fourth saddle branch is monotonically increasing, just as its corresponding minimum. Therefore the intensity of the spatial saddle at the first level is chosen as value for the minimum encapsulating manifold.

Finally an unambiguous hierarchy based on the catastrophe points and the scale space saddles, just as in the 1D case, can be made. The presence of 5 extrema results in 5 inner regions $S_i, i = 1, \ldots, 5$ and a boundary region S_0. The first region is defined by the remaining extremum. The scale space dome defined by this maximum is the iso-intensity manifold valued by the intensity of the extremum at coarsest scale. Since the diffusion equation is energy preserving, this value converges (down) to the average intensity of the initial image. This convergence can also be seen in Figure 7b. The projection of this segment S_1 and its dual S_0 onto the initial image are shown in Figure 8a.

To find the next segment, scale is decreased until the second extremum appears. From the fourth row of Figure 5 it can be seen that this segment S_2 is located at the bottom right part of the image. The value of the iso-intensity manifold is obtained from the scale space saddle of the spatial saddle corresponding to this extremum. The intersection of this manifold with the initial image is shown in Figure 8b. The other segments are found in the same way, resulting in the pre-segmentation of the image as shown in Figure 8f.

This image, although it follows from a well-defined mathematical concept, might be counterintuitive in view of the assumed absence of a small closed region around the

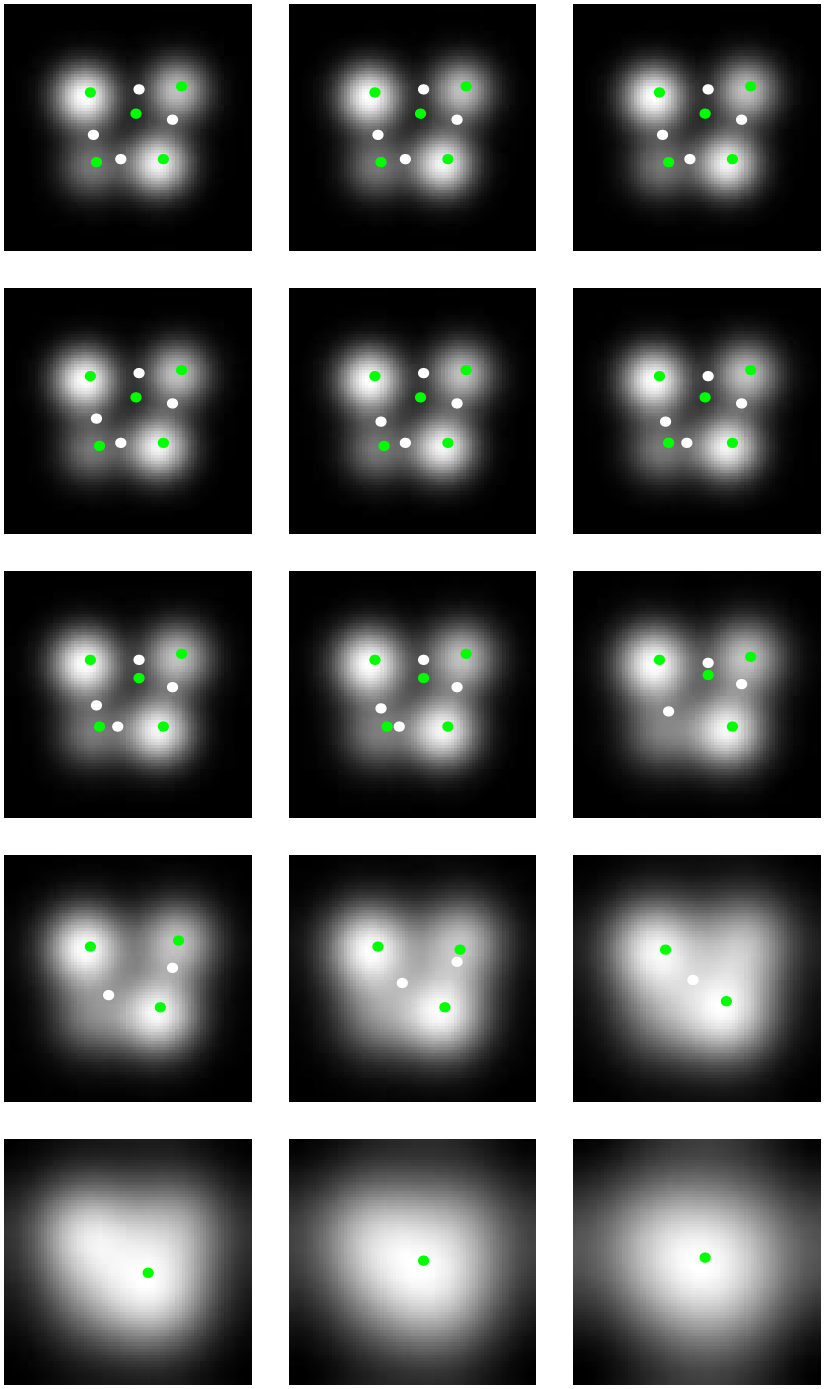

Figure 5: Images from the scale space stack of Figure 4a. Scale increases from left to right, top to bottom. Dark dots denote extrema, bright dots saddle points.

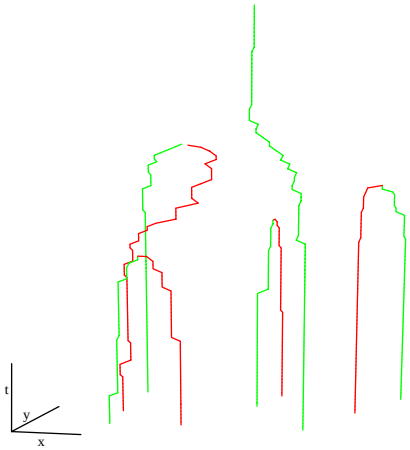

Figure 6: Spatial critical points of Figure 4a in $(x, y; t)$ scale space. Dark grey points correspond to extrema, light grey points to saddle points.

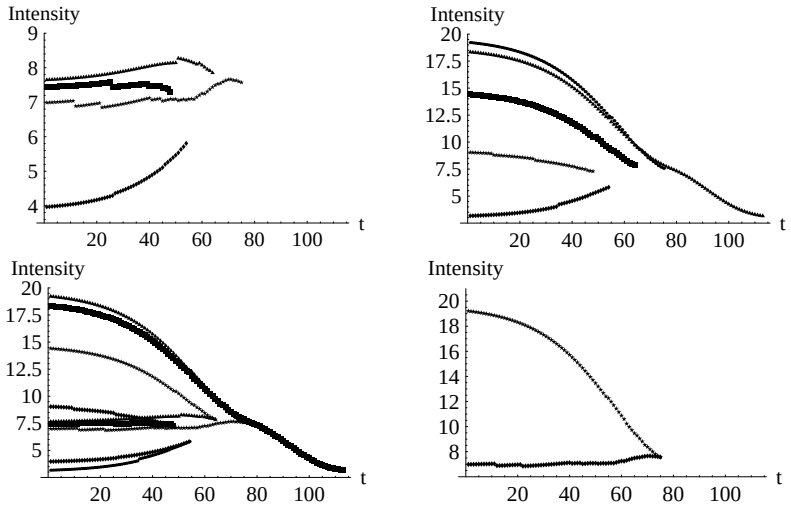

Figure 7: Intensities of the critical paths shown in Figure 6 parametrised by scale. Top-left: Saddle points. top-right: Extrema. bottom-left: All critical points. bottom-right: Saddle-extremum pair.

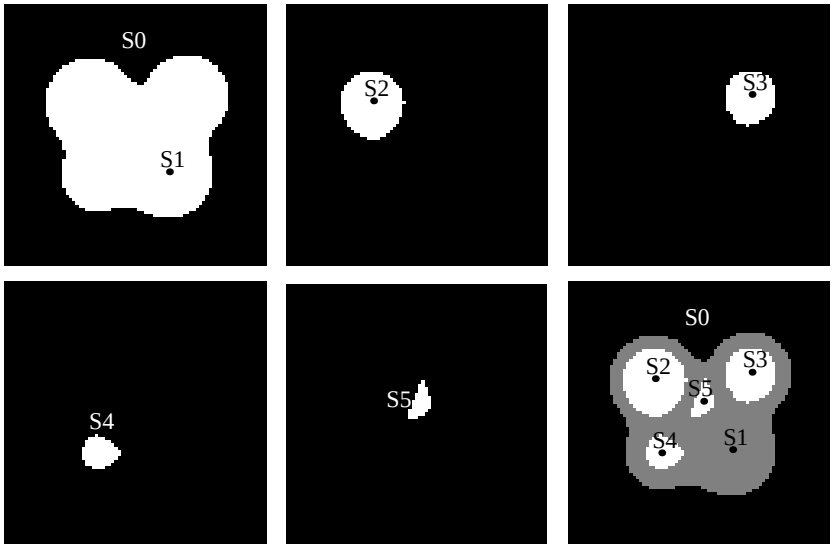

Figure 8: Segments of Figure 4a as defined by the catastrophe points and the scale space saddles. a: Segments S_1 and S_0 projected to the initial image. b: Segment S_2. c: Segment S_3. d: Segment S_4. e: Segment S_5. f: Pre-segmentation of the initial image.

extremum of segment S_1. From Figures 4a and 7b it is clear that this extremum has almost the same intensity as the extremum of segment S_2, so one might expect the size of segment S_1 to be approximately the same as S_2. However, the domes defined by the scale space saddles are nested, so essentially $S_2 \subset S_1$ and from Figure 7 is it clear which saddle-extremum pair annihilates. Although the correct annihilating extrema can be found, it may be desirable – based on prior knowledge of the image and / or of human perceptive characteristics – to add this extra iso-intensity manifold and thus extra segment. In the next section we give an example.

Furthermore, the hierarchy tree associated with this pre-segmentation is given by the successive annihilations in scale space, shown in Figure 9. The nesting of segments is given by $(S_2, S_3, S_4, S_5) \subset S_1$ and the whole image is given by $S_0 \cup S_1$

4.2.2 MR image

Having a hierarchical description tree of the image, one can disregard parts of the tree. Combined with knowledge of the image one can thus obtain a pre-segmentation useful for e.g. further segmentation. Figure 4b shows a 2D slice from a simulated MR brain image.

This input image has 812 extrema and consequently at least 813 separate regions. Obviously, most of these are only defined on a small range of scales. In order to investigate the large structures of this 2D image, we focused on the part of the scale space from scales 8.37 to 33.1, exponentially sampled by 89 scales. The image on scale 8.37, which can be seen in Figure 11a, contains seven extrema of which six annihilate

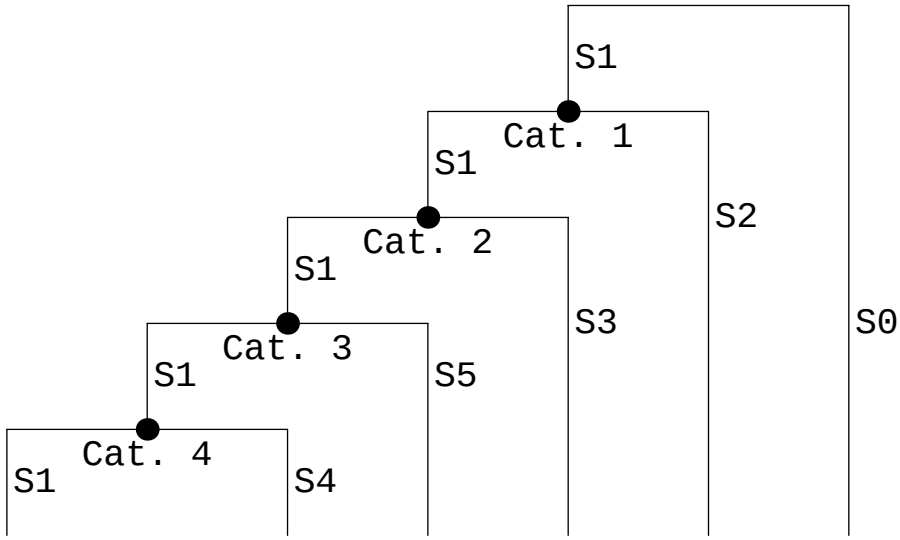

Figure 9: Hierarchy tree of Figure 4a. Segments are labelled corresponding to Figure 8. Segments $S_2, \ldots, S_5$ are subsegments of segment S_1, but annihilate in the sequence S_4, S_5, S_3, S_2 at increasing scale.

in the range unto scale 33.1. The parametrised critical paths in this scale range are shown in Figure 10a, the saddle branches are taken apart in Figure 10b.

The seven extrema define the eight segments of Figure 11b in a similar fashion as in the previous subsection. This pre-segmentation of Figure 11a contains only four levels. The four segments S_1, S_3, S_4, and S_5 correspond to the four maxima located within the most white part of the image. Segment S_2 and its subsegments S_6 and S_7 correspond to the three minima in the interior. The hierarchical structure of this image is shown in Figure 12. To visualise the role of Segment S_1 compared to the other maxima – the part of the tree with catastrophes 2,3, and 4 – the critical intensity of segment S_3 (the adjoined segment by catastrophe 2) was assigned to it. The pre-segmentation with this extra segment is shown in Figure 11c.

As an (other) example of a tree operation on Figure 12, recall that the four segments S_1, S_3, S_4, and S_5 correspond to the four maxima located within the most white part of Figure 11a. We can therefore simplify the tree by clustering these four segments to one region of interest, 'the bright region'. The iso-intensity manifolds have the intensity of the scale space saddle defining segment S_3. Similarly, Segment S_2 and its subsegments S_6 and S_7 correspond to the three minima in the interior of Figure 11a, the dark region in the middle, and can be clustered to one region, 'the dark region'.

The part in scale space bounded by the intensity of the scale space saddles is found by a 3D region growing algorithm. The intersection of the simplified bright and dark region with the initial MR image, Figure 4b, are shown in Figure 13a-b. The pre-segmentation of the initial image with respect to these two parts together with the

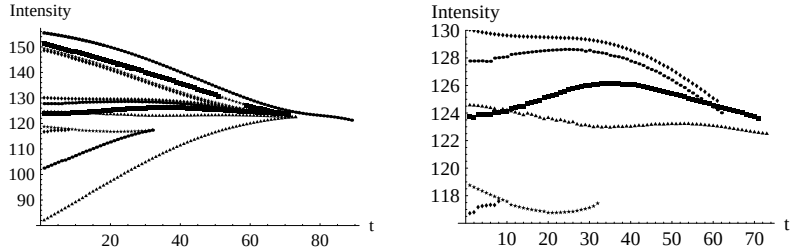

Figure 10: Parametrised intensities of the critical points of the scale space of Figure 11a; 89 scales exponentially sampled from 8.37 to 33.1 Left: All 15 critical points. Right: Intensities of the six spatial saddles.

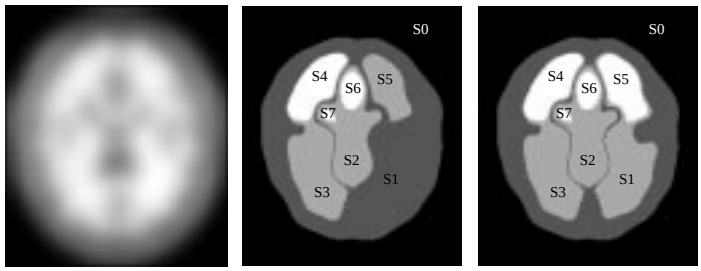

Figure 11: a) MR Image of Figure 4b on scale 8.39. b) Segments of the 7 extrema of a. c) Idem, with the iso-intensity manifold of S_1 chosen equally to S_3.

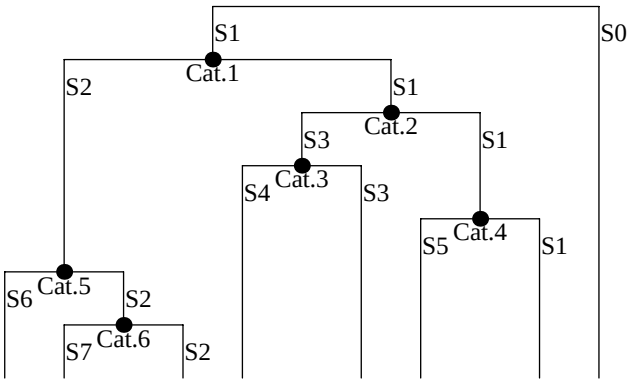

Figure 12: Hierarchy of Figure 11a.

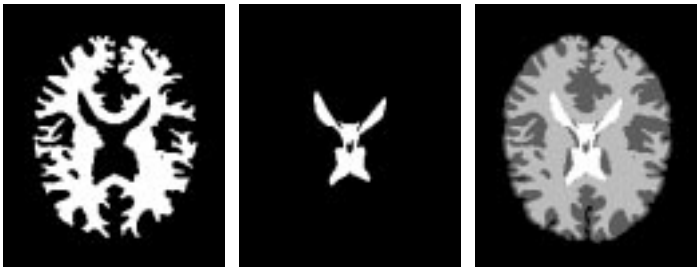

Figure 13: Intersection of the initial image, Figure 4a, with various scale space parts (see text). a) The bright region. b) The dark region. c) Hierarchy simplified to four parts.

segments S_0 and S_1 is shown in Figure 13c.

With the simulated MRI (again shown in Figure 14a), also the probabilistic distributions of the white matter (Figure 14b) and the gray matter (Figure 14c) are given as ground-truth images with values ranging from 0 to 255.

Comparing Figures 13a and 14b shown that the intensity defining the scale space segment of the bright region is a good estimator of the threshold value to the white matter. However, this region is connected whereas the white matter distribution also contains isolated regions. To overcome this difference, we compare the given distributions the initial image thresholded on the values of the scale space saddles.

Figure 14d shows a direct intersection of the original image, Figure 14a, with all the iso-intensity manifolds equalling the intensities of the 7 extrema of the parametrised critical curves. So the range of values is reduced from $0, \ldots, 255$ in the initial image to $0, \ldots, 8$.

The original image thresholded on the intensity defining segment S_3 is shown in Figure 14e. The difference with Figure 13a yields four isolated regions, three in the middle and one in the bottom-right part of the image.

Furthermore, the gray matter can be estimated by subtraction of the bright and the dark regions, as Figure 13c indicates. The original image thresholded on the values of these bright and dark regions is shown in Figure 14f.

To compare the Figures 14b-c with the Figures 14e-f we used the similarity measure of two segments A and B defined by $2\frac{A \cap B}{A+B}$. Since the Figures 14b-c are probabilistic segmentations, they are made binary by thresholding them on the value 128. Then the similarity of the Figures 14b and 14e is 96.6% and of the Figures 14c and 14f is 68.1%. The similarity of the unions of Figures 14b+c and of Figures 14e+f is 89.9%. The error is mainly caused by pixels included only in the segmentation of the ground truth. In other words, Figures 14e and 14f give an underestimation of the probabilistic distributions. The regions found by the tree simplification may be used as an initialisation of a post-processing step to obtain a more accurate segmentation based on the geometry of the image. The latter is obviously not present in the hierarchy tree.

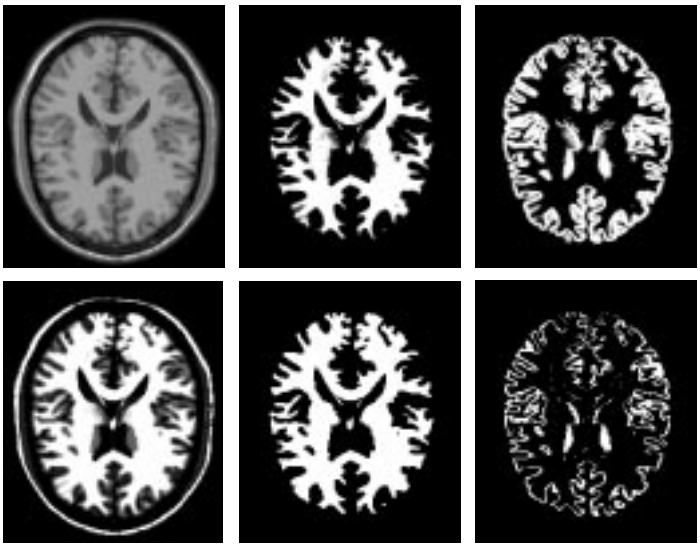

Figure 14: Top row: a) Simulated MR brain image, Figure 4b. b) Ground-truth distribution of white matter. c) Ground-truth distribution of grey matter. Bottom row: d) Segmentation by the isophotes with the value of the 7 extrema. e) Segment thresholded on the value of the bright region. f) Segment thresholded on the values of the bright and dark regions.

5 Conclusions and Discussion

We developed a method to calculate the hierarchical structure of an arbitrary input image. The method is based on the scale space image of the input image and the critical paths within it. The latter exist of branches of spatial extrema and spatial saddle points. The range of scales at which these branches exist follow from their catastrophe points in scale space. These points essentially describe annihilations or creations of pairs of spatial critical points. To each spatial extremum an iso-intensity manifold is assigned. The value of this manifold equals that of the global intensity extremum of the saddle branch that is connected by the annihilation with the extremum branch containing the spatial extremum. This global intensity extremum is located at either the initial scale or at a scale space saddle, a critical point in scale space. The iso-intensity manifold encapsulates the extremum in scale space. The manifolds through the extrema are nested and non-intersecting and thus form a hierarchy.

In contrast to what has been described in the literature we showed that these manifolds necessarily should be chosen such that they go through the scale space saddle instead of the annihilation point.

As application, this structure can be visualised as a pre-segmentation by the intersection of the iso-intensity manifolds with the image at a specified scale or with the input image. The word "pre-segmentation " is chosen, since it is not a task-specified segmentation, but only a division of the image in several topologically defined parts without any a priori knowledge about the contents of the image itself. It may be thus used as an initial segmentation for further post-processing. Other applications may include e.g. clustering and data compression.

The proposed algorithm has two main advantages. Firstly, it has a severe mathematical underpinning which encourages and facilitates future improvements, and admits reproducible, predictable, and provable segmentation results. Secondly, it has the potential to include semantics enabling an intelligent choice of the nodes, either by deterministic, statistic or probabilistic means.

Experimental results based on artificial images and simulated MRI with respect to the hierarchy and pre-segmentation were given. They clarified the theory and showed results that correspond to a fair size to both the mathematical and the intuitive forecast.

A Appendix

We clarify the theory presented in section 2 by discussing the appearance of scale space saddles at the generic catastrophe event in scale space describing an annihilation. This event, called a Fold catastrophe, is known from catastrophe theory (see e.g. [1, 2, 5, 13, 14, 38, 44, 50, 51]) and applied to and used in scale space (see e.g. [8, 9, 10, 12, 20, 21, 22, 23, 24, 31]). Firstly, an example on one-dimensional images is given, because scale space saddles coincide with the catastrophe points. Secondly, the results on a multi-dimensional image is discussed.

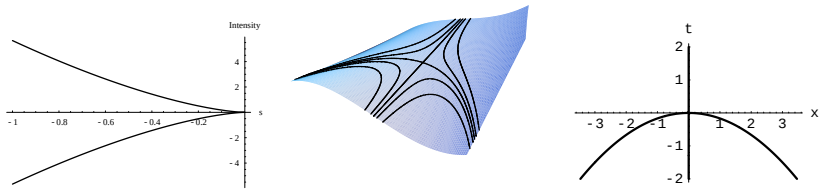

Figure 15: a) Parametrised intensity of a fold catastrophe in 1D with respect to scale. b) $(x, t, L(x;t))$ scale space surface of the fold catastrophe with iso-intensity curves $L(x;t) = c$. c) Segments of b), defined by the scale space saddle intensity $L(x;t) = 0$: for $t < 0$ four segments exist, for $t > 0$ two remain.

1D images

In 1D images the iso-intensity manifolds (or separatrices) are given by the isophotes through the catastrophes points, since these points are identical to the scale space saddles: $H = L_{xx}$ and $L_t = \Delta L = L_{xx}$. The extended Hessian, Eq. (4), reads

$$\mathcal{H} = \begin{pmatrix} 0 & L_{xxx} \\ L_{xxx} & L_{xxxx} \end{pmatrix}.$$

It is generically non-zero at scale space saddles and $\det \mathcal{H} = -L_{xxx}^2 < 0$. The generic annihilation is described by

$$L(x;t) = x^3 + 6xt$$

and has a scale space saddle if both derivatives are zero, that is, $L_x = 3x^2 + 6t = 0$ and $L_t = 6x = 0$. So it is located at the origin with intensity equal to zero. The parametrisation of the critical curve with respect to the scale t is $(x(s); t(s)) = (\pm\sqrt{-2s}; s), s \leq 0$ and the parametrised intensity reads $P(s) = \pm 4s\sqrt{-2s}, s \leq 0$, see Figure 15a. This parametrisation has its local extremum at $s = 0$, the right boundary of the interval on which the branches are defined. An alternative parametrisation of the critical curve, based on the position of the critical points, reads $(x(s); t(s)) = (s; -\frac{1}{2}s^2), \ \forall s$. Then $P_1(s) = -2s^3$ and its critical point $s = 0$ is a point of inflection.

The dome defined by the scale space saddle is given by the isophotes $L(x;t) = 0$ through the origin, so $(x;t) = (0;t)$ and $(x;t) = (x; -\frac{1}{6}x^2)$. Figure 15b shows isophotes in the $(x, t, L(x;t))$-space, where the isophote $L = 0$ gives the annihilation point with the separatrices. The separation curves in the $(x;t)$-plane are shown in Figure 15c.

At the catastrophe point the isophotes of the scale space saddle form a pitchfork. Due to the causality principle it has 3 branches downwards and only one upward, i.e. at the scale space saddle four separate regions change to two separate regions. Locally the isophotes are described by $L(x;t) = L_{xt}(\frac{1}{6}x^3 + xt) \stackrel{\text{def}}{=} 0$, so the horizontal traversing branches of the scale space saddle isophote necessarily have negatively oriented branches by $t = -\frac{1}{6}x^2$.

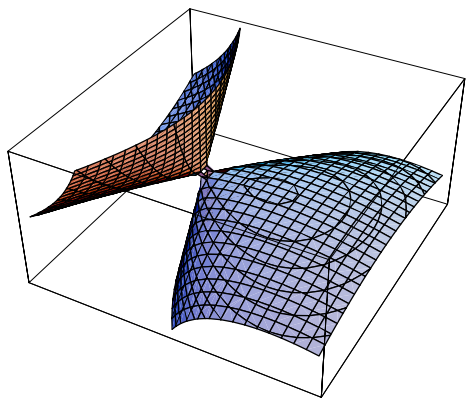

Figure 16: 2D Surface trough a scale space saddle; see text for further details.

n-D images, $n > 1$

In higher dimensions the structure is more complicated, since the scale space saddle does not coincide with the catastrophe point. For n-D images, $n > 1$, it suffices to investigate scale space critical points in 2D, see e.g. [8, 9, 10, 14, 44, 50, 51].

If we assume $L_{yy} = -L_{xx}$ as to satisfy $\Delta L = 0$, the extended Hessian, Eq. (4), becomes

$$\mathcal{H} = \begin{pmatrix} L_{xx} & L_{xy} & L_{xt} \\ L_{xy} & -L_{xx} & L_{yt} \\ L_{xt} & L_{yt} & L_{tt} \end{pmatrix}.$$

The determinant is $-L_{tt}\left(L_{xx}^2 + L_{xy}^2\right) + L_{xx}\left(L_{xt}^2 - L_{yt}^2\right) + 2\, L_{xt}L_{xy}L_{yt}$ and the trace simplifies to L_{tt}, which are both generically non-zero.

The annihilation germ reads

$$L(x, y; t) = x^3 + 6xt + \alpha(y^2 + 2t), \tag{6}$$

where $\alpha = \pm 1$. Positive sign describes a saddle – minimum annihilation, negative sign a saddle – maximum one. Without loss of generality we take $\alpha = 1$. Then $L_x = 3x^2 + 6t$, $L_y = 2y$, $L_t = 6x + 2$, and $\det(H) = 12x$, so the catastrophe takes place at the origin with intensity equal to zero and the scale space saddle is located at $(x, y; t) = (-\frac{1}{3}, 0; -\frac{1}{18})$ with intensity $-\frac{1}{27}$. The surface $L(x, y; t) = -\frac{1}{27}$ is shown in Figure 16. It has a local maximum at $(x, y; t) = (\frac{1}{6}, 0; -\frac{1}{72})$: the top of the extremum dome.

The iso-intensity surface through the scale space saddle can be visualised by two surfaces touching each other at the scale space saddle. One part of the surface is related to the corresponding extremum of the saddle. The other part encircles another -currently unknown- segment of the image. The surface belonging to the extremum forms a dome. The critical curve intersects this surface twice. The saddle branch has an intersection at the scale space saddle, the extremum branch at the top of the dome.

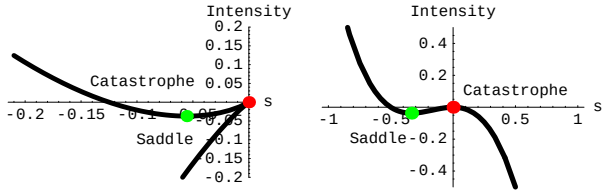

Figure 17: Intensity of the critical curve at fold catastrophe in 2D, parametrised by a) the t-coordinate and b) the x-coordinate. Both show at the origin an annihilation, at the minimum the scale space saddle.

The parametrisation of the critical curve with respect to t (that is: a parametrisation of the branches of the critical curve) is given by $(x(s), y(s); t(s)) = (\pm\sqrt{-2s}, 0; s), s \leq 0$.

The intensity of the critical curve (shown in Figure 17a) then reads $P(s) = 2s \pm 4s\sqrt{-2s}, s \leq 0$, with $\partial_s t(s) = 1$ and $\partial_s P(s) = 2 \pm 6\sqrt{-2s} = \Delta L \cdot t_s(s)$. The critical points of $P(s)$ are given by the scale space saddle, located at $s = -\frac{1}{18}$, and the catastrophe, located at $s = 0$, the boundary of the interval on which the branches are defined. These points are visible in Figure 17a as the local minimum of the parametrisation curve and the connection point of the two curves (a local maximum). The upper branch represents the spatial saddle, the lower one the minimum.

This image led Lifshitz and Pizer [33] to the observation that the intensity of the saddle point decreased even below the annihilation intensity resulting in theoretically problematic linking due to the escape of non-extremum paths from the extremal region they originate in.

This is, however, a generic property of scale space images and shows in an elegant way the necessity of limiting the extremal region by the critical iso-intensity manifold formed by the scale space saddle intensity.

An alternative parametrisation of the critical curve is given by $s = x$, so $(x(s), y(s); t(s)) = (s, 0; -\frac{1}{2}s^2)$, that is: a parametrisation of both branches of the critical curve simultaneously, based on the spatial position of the critical points. Then the intensity of the critical curve is given by $P_1(s) = -2s^3 - s^2$. Now $\partial_s t(s) = -s$ and $\partial_s P_1(s) = -6s^2 - 2s = (6s + 2)(-s)$ and the latter is still equivalent to $\Delta L \cdot t_s(s)$. The critical points of $P_1(s)$ are given by $s = 0$, the catastrophe point, and at $s = -\frac{1}{3}$, the scale space saddle. These points are visible in Figure 17b as the extrema of the parametrisation curve. The branch $s < 0$ represents the saddle point, the branch $s > 0$ the minimum.

References

[1] V. I. Arnold. *Catastrophe Theory*. Springer, Berlin, 1984.

[2] V. I. Arnold, editor. *Dynamical Systems VI: Singularity Theory I*, volume 6 of *Encyclopaedia of Mathematical Sciences*. Springer-Verlag, Berlin, 1993.

[3] J. Blom. *Topological and Geometrical Aspects of Image Structure*. PhD thesis, Utrecht University, 1992.

[4] J. Blom, B. M. ter Haar Romeny, A. Bel, and J. J. Koenderink. Spatial derivatives and the propagation of noise in Gaussian scale-space. *Journal of Visual Communication and Image Representation*, 4(1):1–13, March 1993.

[5] J.W. Bruce and P.J. Giblin. *Curves and Singularities*. Cambridge University Press, 1984.

[6] C.A. Cocosco, V. Kollokian, R.K.-S. Kwan, and A.C. Evans. Brainweb: Online interface to a 3d mri simulated brain database. In *NeuroImage, vol.5, no.4, part 2/4, S425, 1997 – Proceedings of 3-rd International Conference on Functional Mapping of the Human Brain, Copenhagen, May*, 1997.

[7] D.L. Collins, A.P. Zijdenbos, V. Kollokian, J.G. Sled, N.J. Kabani, C.J. Holmes, and A.C. Evans. Design and construction of a realistic digital brain phantom. *IEEE Transactions on Medical Imaging*, 17(3):463–468, 1998.

[8] J. Damon. Local Morse theory for solutions to the heat equation and Gaussian blurring. *Journal of Differential Equations*, 115(2):386–401, 1995.

[9] J. Damon. Generic properties of solutions to partial differential equations. *Arch. Rat. Mech. Anal.*, pages 353–403, 1997.

[10] J. Damon. Local Morse theory for Gaussian blurred functions. In *Sporring et al. [47]*, pages 147–162, 1997.

[11] L. M. J. Florack. *Image Structure*, volume 10 of *Computational Imaging and Vision Series*. Kluwer Academic Publishers, Dordrecht, The Netherlands, 1997.

[12] L. M. J. Florack and A. Kuijper. The topological structure of scale-space images. *Journal of Mathematical Imaging and Vision*, 12(1):65–80, February 2000.

[13] A. T. Fomenko and T. L. Kunii. *Topological Modeling for Visualization*. Springer-Verlag, Tokyo, 1997.

[14] R. Gilmore. *Catastrophe Theory for Scientists and Engineers*. Dover, 1993. Originally published by John Wiley & Sons, New York, 1981.

[15] L. D. Griffin. *Descriptions of Image Structure*. PhD thesis, University of London, 1995.

[16] L. D. Griffin and A. Colchester. Superficial and deep structure in linear diffusion scale space: Isophotes, critical points and separatrices. *Image and Vision Computing*, 13(7):543–557, September 1995.

[17] R. D. Henkel. Segmentation in scale space. In *Computer Analysis of Images and Patterns. Lecture Notes in Computer Science, vol. 970. Springer-Verlag, pages 41-48*, 1995.

[18] T. Iijima. Basic theory of pattern normalization (for the case of a typical oned-imensional pattern). *Bulletin of the Electrotechnical Laboratory*, 26:368– 388, 1962. (in Japanese).

[19] P. Johansen. On the classification of toppoints in scale space. *Mathematical Imaging and Vision*, 4(1):57–67, 1994.

[20] P. Johansen. Local analysis of image scale space. In *Sporring et al. [47]*, pages 139–146, 1997.

[21] P. Johansen, M. Nielsen, and O.F. Olsen. Branch points in one-dimensional Gaussian scale space, 2000.

[22] P. Johansen, S. Skelboe, K. Grue, and J. D. Andersen. Representing signals by their toppoints in scale space. In *Proceedings of the International Conference on Image Analysis and Pattern Recognition (Paris, France, October 1986)*, pages 215–217. IEEE Computer Society Press, 1986.

[23] S. Kalitzin. Topological numbers and singularities. In *Sporring et al. [47]*, pages 181–190, 1997.

[24] S. N. Kalitzin, B. M. ter Haar Romeny, A. H. Salden, P. F. M. Nacken, and M. A. Viergever. Topological numbers and singularities in scalar images. Scale-space evolution properties. *Journal of Mathematical Imaging and Vision*, 9(3):253–296, November 1998.

[25] J. J. Koenderink. The structure of images. *Biological Cybernetics*, 50:363–370, 1984.

[26] J. J. Koenderink. The structure of the visual field. In W. Guttinger and G. Dangelmayr, editors, *The Physics of Structure Formation: Theory and Simulation. Proceedings of an International Symposium, Tubingen, Germany, October 27–November 2 1986*. Springer-Verlag, 1986.

[27] J. J. Koenderink. A hitherto unnoticed singularity of scale-space. *IEEE Transactions on Pattern Analysis and Machine Intelligence*, 11(11):1222–1224, 1989.

[28] J. J. Koenderink and A. J. van Doorn. The structure of two-dimensional scalar fields with applications to vision. *Biological Cybernetics*, 33:151–158, 1979.

[29] J. J. Koenderink and A. J. van Doorn. Dynamic shape. *Biological Cybernetics*, 53:383–396, 1986.

[30] Jan J. Koenderink. *Solid Shape*. MIT Press, Cambridge, Massachusetts, 1990.

[31] A. Kuijper and L.M.J. Florack. Calculations on critical points under gaussian blurring. In *Nielsen et al. [39]*, pages 318–329, 1999.

[32] R.K.-S. Kwan, A.C. Evans, and G.B. Pike. An extensible mri simulator for post-processing evaluation. In *Visualization in Biomedical Computing (VBC'96). Lecture Notes in Computer Science, vol. 1131. Springer-Verlag, pages 135-140*, 1996.

[33] L. M. Lifshitz and S. M. Pizer. A multiresolution hierarchical approach to image segmentation based on intensity extrema. *IEEE Transactions on Pattern Analysis and Machine Intelligence*, 12(6):529–540, 1990.

[34] T. Lindeberg. On the behaviour in scale-space of local extrema and blobs. In P. Johansen and S. Olsen, editors, *Theory & Applications of Image Analysis, volume 2 of Series in Machine Perception and Artificial Intelligence*, pages 38–47. World Scientific, Singapore, 1992.

[35] T. Lindeberg. Scale–space behaviour of local extrema and blobs. *Journal of Mathematical Imaging and Vision*, 1(1):65–99, 1992.

[36] T. Lindeberg. *Scale-Space Theory in Computer Vision*. The Kluwer International Series in Engineering and Computer Science. Kluwer Academic Publishers, 1994.

[37] M. Loog, J.J. Duistermaat, and L.M.J. Florack. On the behavior of spatial critical points under Gaussian blurring. In *Proceedings of the IEEE Workshop on Scale Space and Morphology in Computer Vision, Vancouver, accepted*, 2001.

[38] Y.-C. Lu, editor. *Singularity Theory and an Introduction to Catastrophe Theory*. Springer-Verlag, Berlin, second corrected printing edition, 1976.

[39] M. Nielsen, P. Johansen, O. Fogh Olsen, and J. Weickert, editors. *Scale-Space Theories in Computer Vision*, volume 1682 of *Lecture Notes in Computer Science*. Springer -Verlag, Berlin Heidelberg, 1999.

[40] O. Fogh Olsen. Multi-scale watershed segmentation. In *Sporring et al. [47]*, pages 191–200, 1997.

[41] O. Fogh Olsen and M. Nielsen. Generic events for the gradient squared with application to multi-scale segmentation. In *Ter Haar et al, [49]*, pages 101–112, 1997.

[42] O. Fogh Olsen and M. Nielsen. Multi-scale gradient magnitude watershed segmentation. In *ICIAP'97 - 9th International Conference on Image Analysis and Processing, volume 1310 of Lecture Notes in Computer Science*, pages 6–13, September 1997.

[43] N. Otsu. *Mathematical Studies on Feature Extraction in Pattern Recognition*. PhD thesis, Electronical Laboratory, Ibaraki, Japan, 1981. (in Japanese).

[44] T. Poston and I. N. Stewart. *Catastrophe Theory and its Applications*. Pitman, London, 1978.

[45] J.H. Rieger. Generic evolutions of edges on families of diffused greyvalue surfaces. *Journal of Mathematical Imaging and Vision*, 5:207–217, 1995.

[46] A. Simmons, S.R. Arridge, P.S. Tofts, and G.J. Barker. Application of the extremum stack to neurological MRI. *IEEE Transactions on Medical Imaging*, 17(3):371–382, June 1998.

[47] J. Sporring, M. Nielsen, L.M.J. Florack, and P. Johansen, editors. *Gaussian Scale-Space Theory*, volume 8 of *Computational Imaging and Vision Series*. Kluwer Academic Publishers, Dordrecht, second edition, 1997.

[48] B. M. ter Haar Romeny, editor. *Geometry-Driven Diffusion in Computer Vision*, volume 1 of *Computational Imaging and Vision Series*. Kluwer Academic Publishers, Dordrecht, 1994.

[49] B. M. ter Haar Romeny, L. M. J. Florack, J. J. Koenderink, and M. A. Viergever, editors. *Scale-Space Theory in Computer Vision: Proceedings of the First International Conference, Scale-Space'97, Utrecht, The Netherlands*, volume 1252 of *Lecture Notes in Computer Science*. Springer-Verlag, Berlin, July 1997.

[50] R. Thom. *Stabilité Structurelle et Morphogénèse*. Benjamin, New york, 1972.

[51] R. Thom. *Structural Stability and Morphogenesis*. Benjamin-Addison Wesley, 1975. translated by D. H. Fowler.

[52] K.L. Vincken, A.S.E. Koster, and M.A. Viergever. Probabilistic multiscale image segmentation. *IEEE Transactions on Pattern Analysis and Machine Intelligence*, 19(2):109–120, 1997.

[53] T. Wada and M. Sato. Scale-space tree and its hierarchy. In *ICPR90*, pages Vol–II 103–108, 1990.

[54] J. Weickert. *Anisotropic Diffusion in Image Processing*. Teubner, Stuttgart, 1998.

[55] J.A. Weickert, S. Ishikawa, and A. Imiya. On the history of Gaussian scale-space axiomatics. In *Sporring et al, [47]*, 1997.

[56] J.A. Weickert, S. Ishikawa, and A. Imiya. Linear scale-space has first been proposen in Japan. *Journal of Mathematical Imaging and Vision*, 10(3):237–252, 1999.

[57] A.P. Witkin. Scale-space filtering. In *Proceedings of the Eighth International Joint Conference on Artificial Intelligence*, pages 1019–1022, 1983.

[58] N. Zhao and T. Iijima. A theory of feature extraction by the tree of stable viewpoints. *IECE Japan, Trans. D*, J68-D:1125–1132, 1985. (in Japanese).